Chapter 4

Selected Sources in the Small Magellanic Cloud

4.1 Introduction

The ATCA observations of the selected sources in the SMC do not concentrate on a single class of source, but rather those expected on the basis of earlier surveys to be interesting or whose nature was uncertain. The MOST 843 MHz survey observations of the SMC were used to select the sources based mainly on morphology, flux density and position. The environment surrounding the source of interest was also noted.

In this chapter, both the MOST and ATCA images are presented along with comparison with existing published data from optical, radio and infrared observations. One of the aims of the SMC work is to classify the sources into a small number of distinct categories, and then use these as the basis for studying the larger sample of sources in the Large Magellanic Cloud discussed in Chapter 5. Spectral index considerations, source identification and a comparison with the expected number of background sources is also covered in this Chapter.

4.2 Observations of Selected SMC Sources

Details of the ATCA observations of the SMC are provided in Table 3.1.

4.2.1 The "BKGS" X-ray Sources

Four sources which were catalogued as low quality detections by Bruhweiler et al. (1987), hereafter referred to as BKGS, were observed as part of this programme. Only a single ATCA configuration was used for each of the sources. The X-ray observations were obtained using the low-resolution Image Proportional Counter (IPC) on-board the *Einstein* satellite. This permitted large areas to be observed quickly; in the best case the IPC has an angular resolution of around 30 arcsec. BKGS do not quote the 90% confidence X-ray error radius for the four sources studied here.

These four BKGS sources were chosen because the MOST images showed relatively compact sources with a reasonably strong flux density with positions coincident with the X-ray position. The coincidence of radio emission and possible X-ray emission suggests the possible detection of non-thermal emission which could be associated with a previously unknown supernova remnant.

Table 4.1: Comparison of the MOST 843 MHz and ATCA 4790 MHz observations of the BKGS sources in the Small Magellanic Cloud with published Parkes Survey Data. The reference column indicates if the tabulated data were taken from a published survey. B1950.0 positions are quoted if these are listed in the published catalogues; such positions have been precessed to obtain corresponding J2000.0 positions for the purposes of comparison.

Source	Frequency (GHz)	Source Position (B1950.0)	Source Position (J2000.0)	Integrated Flux Density (mJy)	Reference
BKGS 7					
X-ray	–	00 51 39 –72 52 11	00 53 24 –72 35 55	–	BKGS
MOST #1	0.843		00 53 20.46 –72 35 36.1	53	
BKGS 24					
X-ray	–	01 15 09 –73 30 34	01 16 30 –73 14 46	–	BKGS
MOST #1	0.843		01 16 28.65 –73 14 38.1	143	
ATCA #1	4.79		01 16 28.91 –73 14 38.8	10	
BKGS 32					
X-ray	–	01 19 40 –73 51 00	01 20 55 –73 35 18	–	BKGS
MOST #1	0.843		01 20 54.23 –73 34 56.8	66	
ATCA #1	4.79		01 20 56.05 –73 34 53.3	16	
B0119–7350	4.85	01 19 47.6 –73 50 03	01 21 02.8 –73 34 22	41	Filipovic
BKGS 33					
X-ray	–	01 25 32 –73 43 06	01 26 42 –73 27 33	–	BKGS
MOST #1	0.843		01 26 29.31 –73 27 13.8	62	
ATCA #1	4.79		01 26 29.25 –73 27 14.3	12	

BKGS 7 The source catalogued as BKGS 7, was not detected with the ATCA and thus no image is presented. The image obtained with the MOST at 843 MHz is shown in Figure 4.1. This image also contains a source associated with the field 0050–727 discussed later in this chapter. The BKGS 7 detection was classified by BKGS to be of Quality C (with A being the highest and D the lowest) indicating that a source was detected with two different versions of software but is only marginally detected in a visual inspection of the X-ray field.

BKGS 24 This source is also classified as a Quality C detection. The ATCA image of this region is shown in Figure 4.2. The MOST image of this source is contained in the 0119–731 field and is shown in Figure 4.5 (located in the section on H II regions).

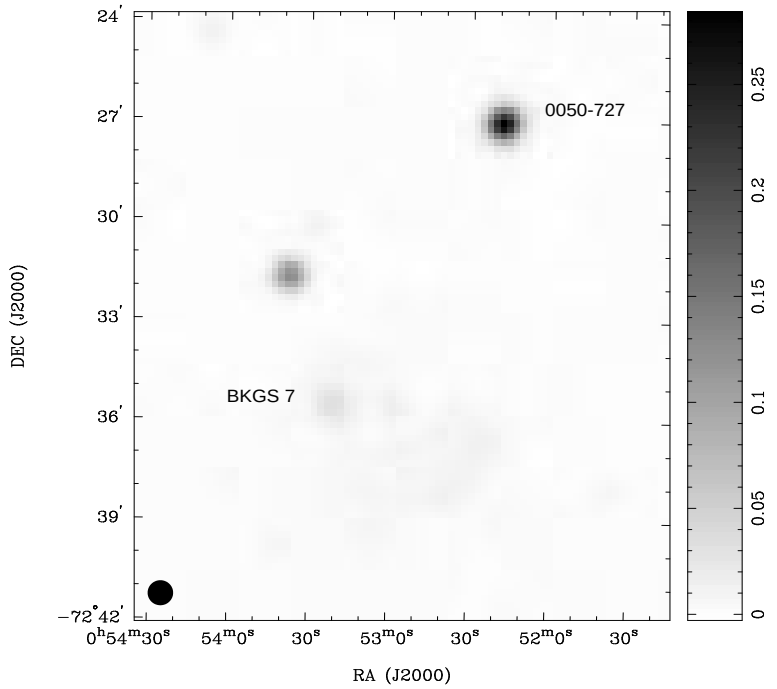

Figure 4.1: The MOST 843 MHz total intensity image of BKGS 7 and 0050–727. The radio source associated with BKGS 7 is the faint source located in the lower-left quadrant of the image. There is also extended diffuse emission in the lower half of the image which is more easily seen on a workstation display. The source associated with 0050–727 is the strong compact source located in the north-west quadrant. The intensity units are in Jy/beam. The wedge to the right of the image gives an indication of the transfer function. The HPBW is shown in the lower-left corner.

This field also contains the known H II region SMC N83/N84 which is discussed later in this Chapter. The possible X-ray source has a position determined by BKGS as:

01 15 09 –73 30 34 (B1950.0) or 01 16 30 –73 14 46 (J2000.0).

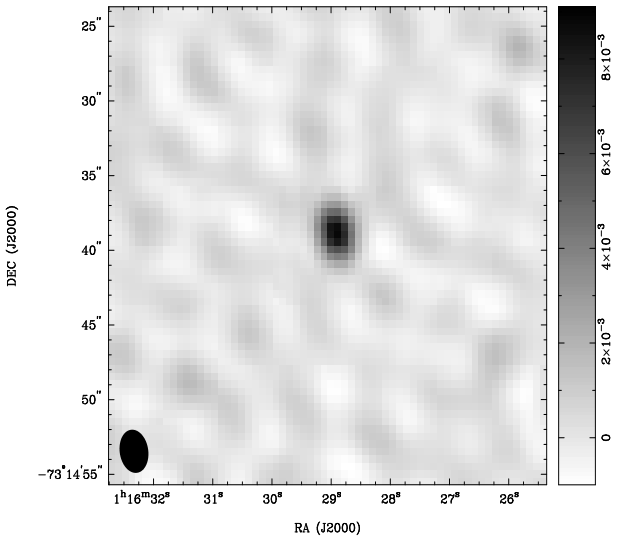

Figure 4.2: The ATCA 4790 MHz total intensity image of the region near BKGS 24. The intensity units are in Jy/beam. The wedge to the right of the image gives an indication of the transfer function. The HPBW is shown in the lower-left corner.

The source fit to the ATCA data is given in Table 4.1. The nominal difference between the position of the X-ray source and the radio source suggests that the source detected with the MOST and ATCA may be associated with the possible X-ray source. It also must be recognised that as the *Einstein* IPC detector has an angular resolution of around 30 arcsec the determination of X-ray positions for comparison purposes is difficult. However, this source was not detected in any of the recent Parkes radio surveys or the recent *ROSAT* X-ray survey. Although it is difficult to say with any certainty if the radio and X-ray sources are the same source, the low-quality X-ray detection suggest that this may be none other than a background radio source that appears approximately coincident with the X-ray position. An alternative possibility is that any X-ray emission may be from a background AGN. From the MOST and ATCA radio data the spectral index is around -1.5. This spectral index can be considered as being characteristic of a steep spectrum background source.

BKGS 32 This is also catalogued as being of Quality C. The MOST image is shown on the left of Figure 4.3 and the corresponding ATCA image of this region on the right-hand side of the same figure. The source position given by BKGS is:

01 19 40 –73 51 00 (B1950.0) or 01 20 55 –73 35 18 (J2000.0).

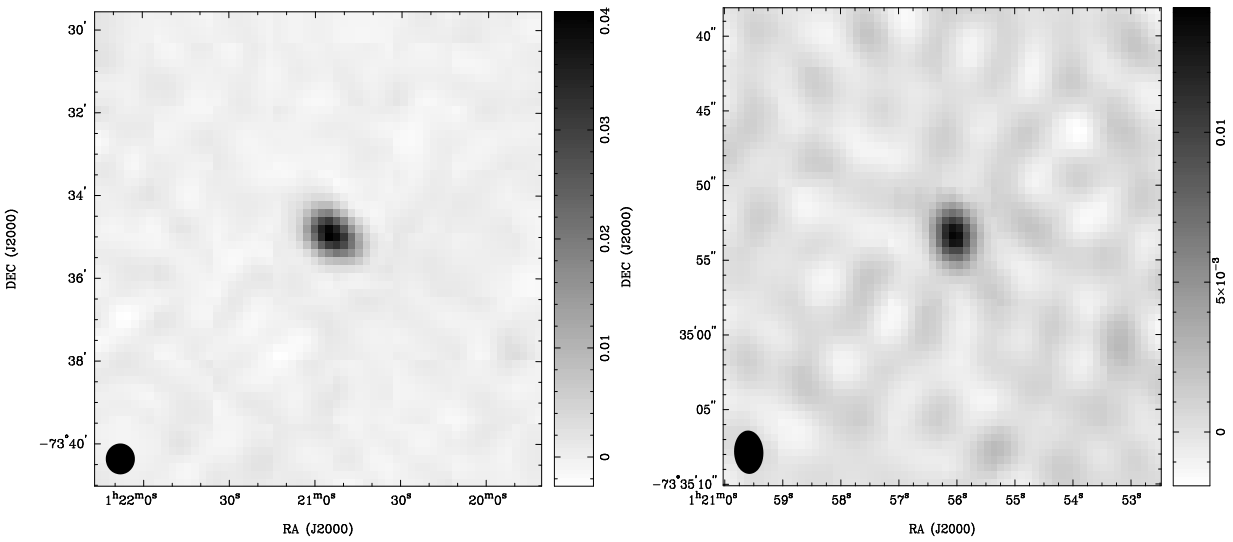

Figure 4.3: The MOST 843 MHz (left) and ATCA 4790 MHz (right) total intensity images of the region near BKGS 32. The intensity units are in Jy/beam. Note the very different scales of the two images.

The ATCA position is given in Table 4.1. There seems to be a good correlation between the MOST and ATCA determined positions and that published by BKGS so it is likely this source is associated with the possible X-ray detection. In addition, Filipovic et al. (1998b), gives a flux density of 41 mJy at 5 GHz for a source located at RA = 01 19 47.6, Dec = –73 50 03 (B1950.0) and they identify this source as being BKGS 32. There is some discrepancy between the flux density determined from the Parkes data and the ATCA observations. However, given the difference between the effective beam widths, it is probable that the Parkes result includes contributions from other sources within the beam and so is an overestimate or that the ATCA is under-sampling the flux density due to incomplete spatial frequency coverage leading to an underestimate.

Taking the MOST and ATCA data, the spectral index is calculated as -0.8 which suggests the possibility of non-thermal emission and supports the possibility that there is X-ray emission. The source morphology doesn't provide any additional information as to the nature of the source. Thus the source categorization is somewhat uncertain; it may be an SNR (based on the non-thermal radio spectrum and low-quality X-ray detection) or more likely a background source.

BKGS 33 This BKGS source was rated to be of the lowest quality, D, and included in their catalogue for "the sake of completeness". The X-ray detection was flagged solely via software; no source is visible by inspection of the images. The source position determined by BKGS is:

01 25 32 –73 43 06 (B1950.0) or 01 26 42 –73 27 34 (J2000.0),

The MOST and ATCA images are shown in Figure 4.4 and both clearly indicate the presence of a radio source. The ATCA source position is given in Table 4.1. Given the

uncertainty in the X-ray position and low quality detection of the source, it is difficult to be certain that this radio source is the same source detected at X-ray wavelengths. A comparison with published catalogues indicates that this source was not detected in the Parkes multi-frequency radio surveys or the *ROSAT* X-ray survey of the SMC.

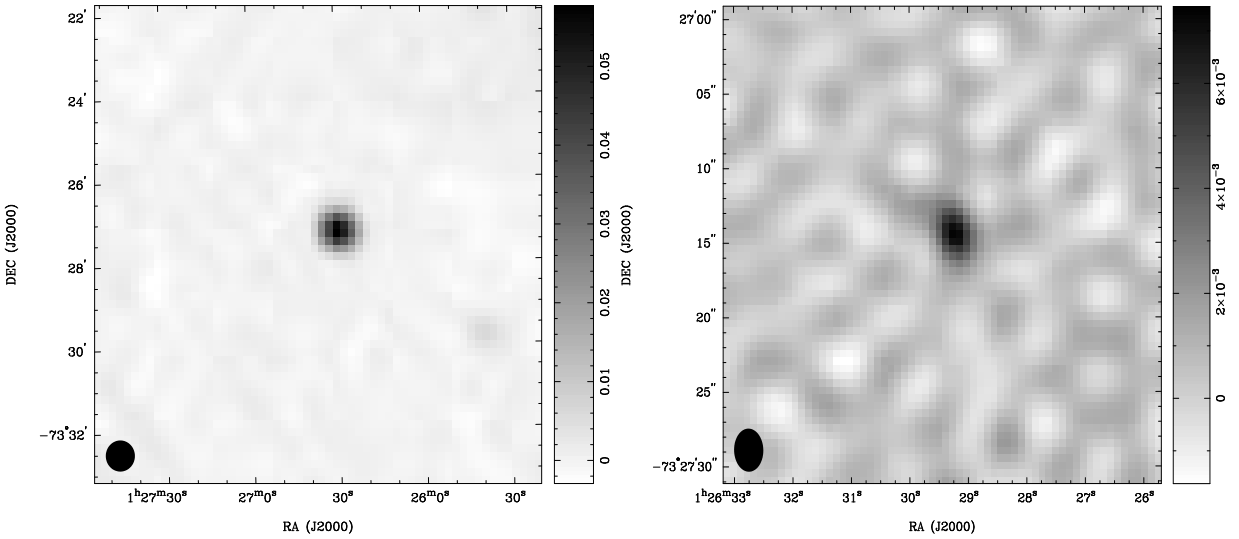

Figure 4.4: The MOST 843 MHz (left) and ATCA 4790 MHz (right) total intensity images of the region near BKGS 33. The intensity units are in Jy/beam.

There are at least two nearby sources listed in Filipovic et al. (1998b), B0124-7339 and B0125-7331, but one is identified as the known H II region N89 (Henize 1956) and the second is classified as a background source. Neither of these sources is sufficiently close to the ATCA determined position to be the same object. A spectral index of -1.0 was calculated from the MOST and ATCA data which is suggestive of a steep spectrum background source. The X-ray emission, if it was detected, could be associated with a background AGN.

4.2.2 The H II Regions SMC N83/N84 and SMC N90

These H II regions were first catalogued on the basis of optical studies by Henize (1956) and subsequently in the Davies, Elliott & Meaburn (1976) survey. By their nature, the thermal emission process means that they have a relatively flat spectrum (typically $\alpha > -0.2$ where α is defined by $S \propto \nu^{+\alpha}$) at centimetre wavelengths and hence have been detected in numerous Parkes surveys. The motivation behind the higher resolution ATCA observations was to determine the presence of and to image any compact components (such as an SNR), that may be associated with the H II region. The relatively short observing programme was unlikely to image the large scale structure of the H II nebula.

As noted in Table 3.1 these sources were observed on a number of different dates in various baseline configurations. This was advantageous in that a range of spatial frequencies were sampled, as shown for the observations of SMC N83/N84, in Figure 3.1.

Hence this should result in high quality images from which a relatively accurate determination of integrated flux density can be made.

SMC N83/N84 The MOST image is shown in Figure 4.5. The radio emission from the H II region is composed of a number of discrete sources and diffuse emission in the right half of the image. The strong, compact source to the upper-left is the radio source possibly associated with the X-ray source BKGS 24 discussed earlier.

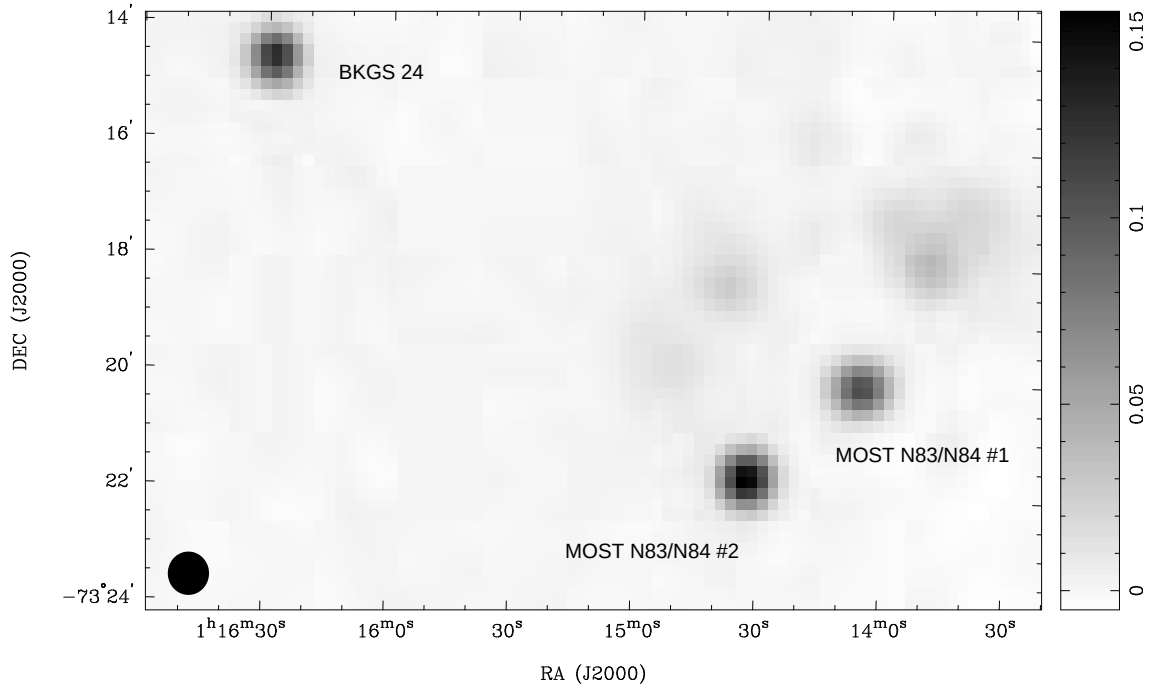

Figure 4.5: The MOST 843 MHz total intensity image of BKGS 24 (which is the source located in the upper-left corner of the image) and the known H II region SMC N83/N84 (the cluster of sources on the right side of the image). The intensity units are in Jy/beam.

Two sub-images from the single ATCA observed field centered on N83/N84 are shown in Figure 4.6. Careful analysis of the first ATCA image suggests that there are two fainter sources to either side of the stronger source in the centre of the field. It is possible that these may be artifacts of the imaging process or of an instrumental problem affecting the data. However, we believe these two weaker sources to be real for three reasons. Firstly, the MOST image suggests that there are a number of discrete sources co-located with this H II region. Secondly, these weaker sources are not visible in the second ATCA image (taken from the same dataset). Third, care was taken during the observation and data reduction phases, such as shifting the observed field centre away slightly from the source position and removing any suspect visibility data.

The strong source in the first of the two ATCA images corresponds to the weaker of the two source on the right-hand side of the MOST image. The second ATCA image

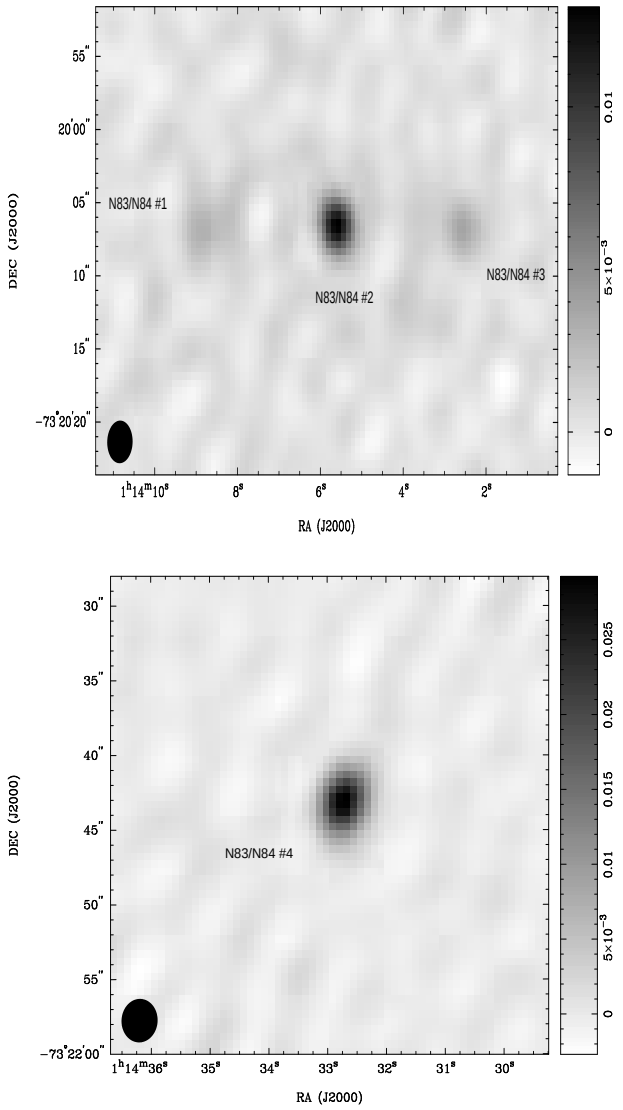

Figure 4.6: The ATCA 4790 MHz total intensity images of sources in the vicinity of the SMC H II regions N83 and N84. Note that the larger-scale diffuse emission is essentially resolved out in these observations. The intensity units are in Jy/beam.

is of the strong compact source at the southern edge of the MOST image. Positional agreement between the MOST and ATCA positions (as determined using the same fitting procedure) is very good.

Source parameters as determined from fitting all four sources detected in these ATCA observations are given in Table 4.2. Direct comparison of these sources with the Parkes multi-frequency surveys is difficult because at most frequencies the source in the Parkes catalogues is marked as being extended. Given the beam-width of the Parkes antenna at centimetre wavelengths (e.g. at a frequency of 5 GHz, the HPBW is around 4.5 arcmin), the Parkes surveys will be sensitive to regions of extended emission. Certainly, the first three sources listed are all contained in the first image of Figure 4.6 would clearly not be resolved as discrete sources in the Parkes surveys.

Filipovic et al. (1998b) associate the source B0112–7333 with the H II region N83. There was a definite detection in the 20, 13, 6 and 3 cm bands at Parkes with the source marked as extended at all frequencies except for 2.45 GHz. This seems an anomaly as it would be reasonable to assume that an emission nebula would be extended at all frequencies within this range, particularly when the source is listed as extended at all other observed frequencies. The conversion of catalogued B1950.0 coordinates of both the 4.75 GHz position (similar frequency to these ATCA observations) and also the 8.55 GHz position (this has the highest angular resolution and should thus have the most accurate position) are given in Table 4.2.

Table 4.2: Comparison of the MOST 843 MHz and ATCA 4790 MHz observations of two H II regions in the Small Magellanic Cloud with published survey data from Parkes and X-ray observations. The reference column indicates if the tabulated data was taken from a published survey. B1950.0 positions are quoted if these are listed in the published catalogues; such positions have been precessed to obtain corresponding J2000.0 positions for the purposes of comparison.

Source	Frequency (GHz)	Source Position (B1950.0)	Source Position (J2000.0)	Integrated Flux Density (mJy)	Reference
SMC N83/N84					
MOST #1	0.843		01 14 05.31 –73 20 05.8	134	
MOST #2	0.843		01 14 32.42 –73 21 42.4	177	
ATCA #1	4.79		01 14 08.68 –73 20 06.6	16	
ATCA #2	4.79		01 14 05.59 –73 20 06.5	18	
ATCA #3	4.79		01 14 02.57 –73 20 06.7	8	
ATCA #4	4.79		01 14 32.72 –73 21 43.1	40	
B0112–7333	4.75	01 12 59.5 –73 33 32	01 14 22.3 –73 17 40	50	Filipovic
B0112–7333	8.55	01 12 17.5 –73 33 11	01 13 41.0 –73 17 19	40	Filipovic
BKGS 22	–	01 12 43 –73 35 30	01 14 06 –73 19 40	–	BKGS
B0113–7334	8.55	01 13 07.9 –73 34 52	01 14 30.5 –73 19 01	38	Filipovic
RXJ0114.2–7319	–	01 12 49.7 –73 35 35	01 14 12.5 –73 19 43	–	Kahabka
BKGS 23	–	01 14 32 –73 35 08	01 15 53 –73 19 19	–	BKGS
SMC N90					
MOST #1	0.843		01 29 30.23 -73 33 10.9	214	
ATCA #1	4.79		01 29 30.18 –73 33 10.5	73	
B0128–7348	4.75	01 28 23.1 –73 48 40	01 29 30.5 –73 33 12	147	Filipovic

Comparing these positions with those determined from the ATCA, it is difficult to be certain that the catalogued and identified source N83/N84 in the Parkes surveys is one (or all) of the three sources on the ATCA image. Although the Parkes observations would have a significant contribution from the emission nebula and probably only a small contribution (if any) from objects behind the SMC it may be that these sources are related. It is reasonable to conjecture that the compact sources in the first of the two ATCA images are background to the SMC, apparently coincident with the H II region. Any extended emission has been essentially resolved out in these ATCA observations.

Source 22 in the BKGS survey may be related to N83/N84. The position in both B1950.0 (as published) and J2000.0 is given in Table 4.2. Although catalogued as a very low quality detection (Quality D), given the position uncertainty it could be argued that this source may be associated with the emission nebulae and associated radio sources. No source in this area was detected in the more recent *ROSAT* survey by Kahabka et al. (1999). Given that H II regions typically do not exhibit X-ray emission, that the BKGS detection had the lowest quality rating, and that no X-ray source was detected in the *ROSAT* survey, it is unlikely that there is an X-ray source associated with N83/N84 in the SMC.

The position of the source on the second ATCA image (named as N83/N84 #4) is given in Table 4.2. This apparently corresponds to a source B0113–7334 detected at 8.55 GHz in the Parkes multi-frequency surveys (Filipovic et al. 1997). The position of the Parkes source is given in Table 4.2, it has a flux density at this frequency of 383 mJy and is categorized as "extended". This relatively strong source at 8.55 GHz was not detected at the lower frequencies in the Parkes surveys, for reasons that are unclear. Given that this source is within 3 arcmin of the ATCA 5 GHz sources position it is likely that both positions refer to the same object. The *ROSAT* X-ray survey of Kahabka et al. (1999) identifies the source RXJ0114.2–7319 with this H II region; the position is given in Table 4.2. There is also some suggestion that X-ray source BKGS 23, rated as being a very low quality detection, may be associated with this H II region. Although the position agreement in declination is very good there is a significant offset in right ascension. Based on these results, it would appear that the source N83/N84 #4 may be background to the SMC, apparently coincident with the H II region.

SMC N90 The MOST and ATCA images of this source are shown in Figure 4.7. The MOST image shows a compact source with fainter extended emission surrounding this feature. There is a suggestion of a weaker but nonetheless compact source just to the north-east of the central strong source. The only significant feature in the ATCA image is a relatively strong and compact source. As is the case for the images of N83/N84 any large-scale diffuse emission would be resolved out at the resolution of the ATCA. The parameters of the compact source are given in Table 4.2.

The Parkes surveys at 1.42 GHz, 2.45 GHz, 4.75 GHz and 4.85 GHz (the latter as part of the PMN survey (Wright et al. 1994)) all detected radio emission in this field. Designated B0128–7348, the details of this source at 4.75 GHz are given in Table 4.2.

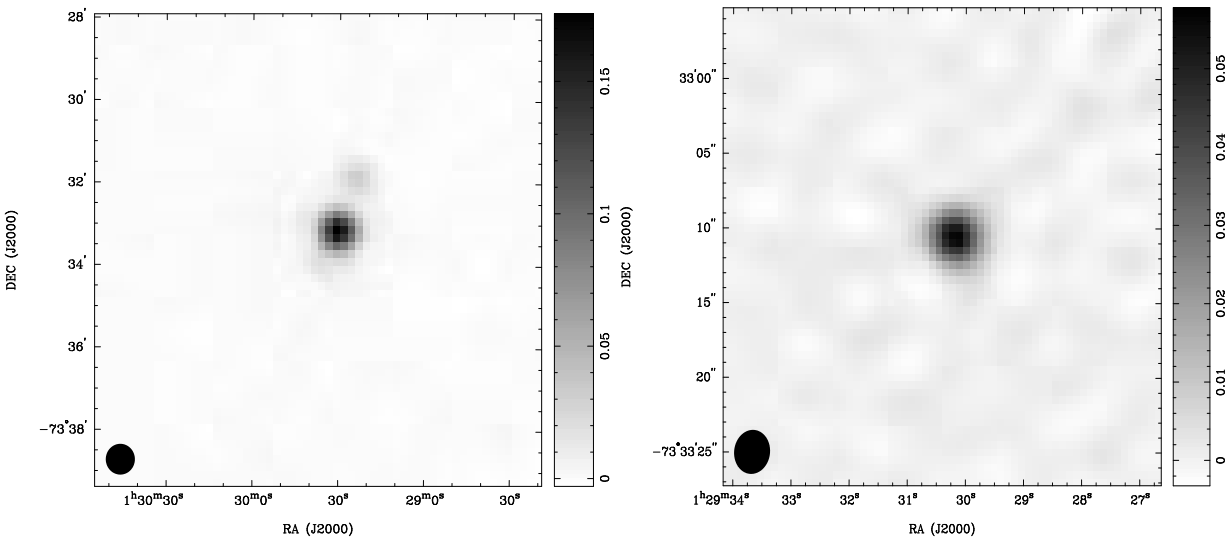

Figure 4.7: The MOST 843 MHz (left) and ATCA 4790 MHz (right) total intensity images of a strong, compact source near the SMC H II Region N90. The intensity units are in Jy/beam. Note the weak compact source to the north-west of the MOST image.

The Parkes source is not classified as "extended" at any of these frequencies, and its position is in excellent agreement with the MOST and ATCA positions obtained in this work. The Parkes source was identified as being N90, although it would be difficult to determine from the Parkes observations the contribution from the thermal emission nebula and any compact component as seen in the higher-resolution radio images. Furthermore, there was no detection of coincident emission in any of the X-ray surveys. Therefore, although it is conceivable that the compact source imaged with the MOST and ATCA is associated with the H II region, it is more likely that it is a background source coincident with the emission nebula.

4.2.3 Other Compact Sources in the Direction of the SMC

0021−742 The MOST and ATCA images of the sources of interest in this field are shown in Figure 4.8 and Figure 4.9 respectively. The MOST image shows two nearby compact sources, each surrounded by some fainter diffuse emission. The weaker of the two MOST sources to the south-east corresponds to the first of the two ATCA images. The stronger MOST source to the north-west corresponds to the second of the ATCA images and is more interesting from a morphological perspective.

The ATCA image of source #1 in Figure 4.9 shows a relatively compact source with a possible faint extension to the north-west and west, which may or may not be related to the compact source. The image of ATCA source #2 shows a compact source and an extended half-ring of emission to the north-east. Both the compact source and the extended half-ring appear to be sitting on a roughly circular area of diffuse emission. The coincidence of the compact source with the continuation of the ring may imply

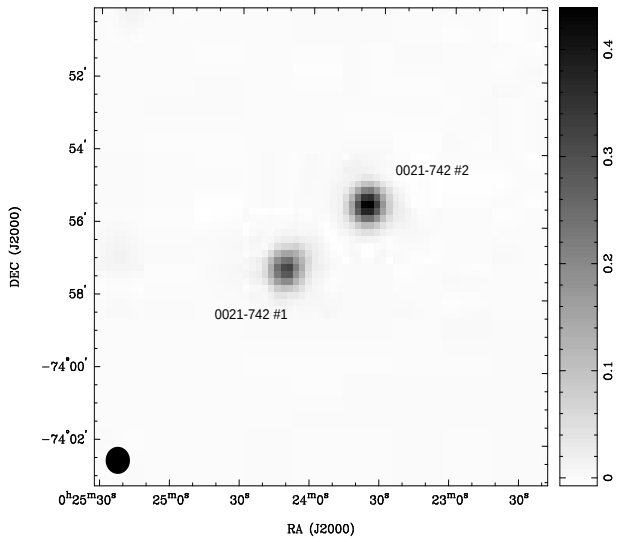

Figure 4.8: The MOST 843 MHz total intensity image of the field 0021–742 in the Small Magellanic Cloud. The intensity units are in Jy/beam.

that the two are part of the same object, but it is possible that the compact source is unrelated to the area(s) of extended emission. The latter has a morphology that is strongly suggestive of the partial-shell of a supernova remnant.

Source fitting routines that rely on fitting a simple gaussian to a region of emission which exceeds a pre-determined noise threshold do not provide meaningful results for extended sources of non-gaussian morphology. The source fit for ATCA source #2 has therefore only considered the compact component on the western side of the image. The fitting procedure gives an integrated flux density for this component of approximately 17 mJy. A reasonable estimate of the total flux density can be determined by interactively selecting the region of interest using the *MIRIAD* routine `cgcurs`. If the diffuse emission and the compact source are treated together, the integrated flux density is around 73 mJy. Excluding the compact source gives a figure around 47 mJy. The formal fitting procedure will probably have over estimated the flux density of the compact component because of the nearby extended emission. Given this and other considerations the values are relatively self-consistent.

The nearest source to 0021–742 #1 detected in the Parkes surveys is B0022–7403. This source was only detected at 4.85 GHz as part of the PMN survey, and not by the multi-frequency work reported in the various papers by Filipovic. It is highly unlikely that ATCA source 0021–742 #1 and B0022–7403 are the same object given the position difference of over 10 arcmin in declination. There is also no detected X-ray or infrared emission at or near ATCA source 0021–742 #1. The faint extension of ATCA source 0021–742 #1 to the north-west may indicate that it is located in the Clouds. Alternatively, the extended emission may be in the Clouds while the compact component is a coincident background source. Data at other wavelengths are needed before it will be possible to be confident as to the nature of this source.

The Parkes source B0021–7412, has a similar position to ATCA 0021–742 #2 and

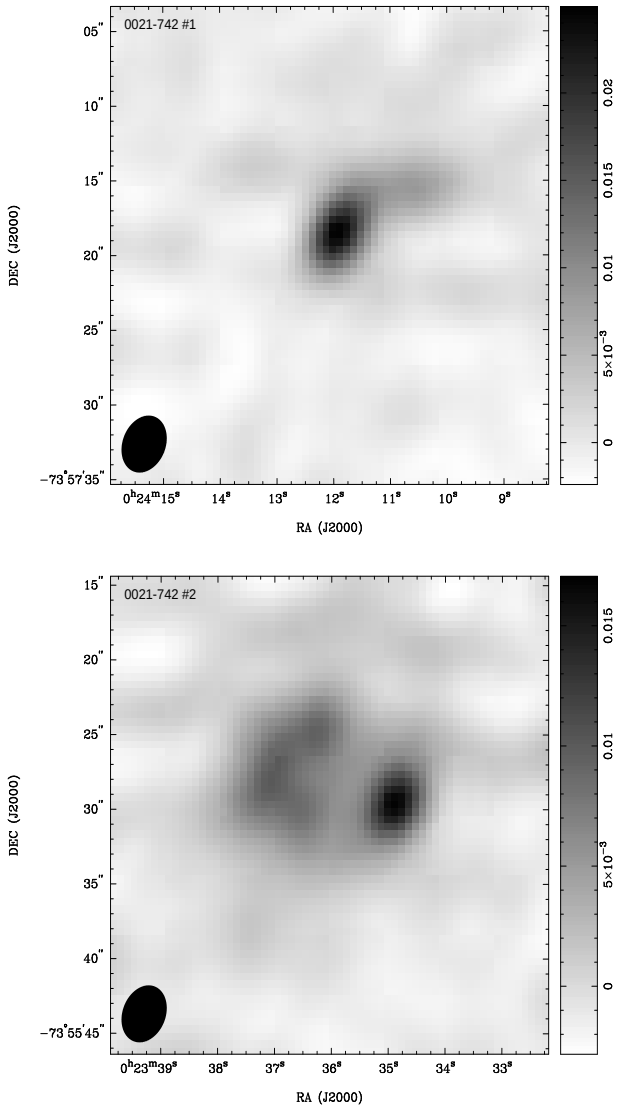

Figure 4.9: The ATCA 4790 MHz total intensity images of 0021-742 in the Small Magellanic Cloud. The intensity units are in Jy/beam.

was detected at all frequencies (see Table 4.3). None of the Parkes surveys have sufficient angular resolution to distinguish between the compact source to the west of the image and the more diffuse extended emission to the north-east. The Parkes beam at centimetre wavelengths would contain the contribution to the flux density from these sources and also from any other emission within the area covered by the beam. B0021–7412 is classified by Filipovic et al. (1998b) as being a background source. No coincident X-ray or infrared emission has been detected.

The observations are consistent with a number of scenarios for the nature of ATCA source 0021–742 #2. The extended partial ring is an improbable morphology for a background source and is likely to be located in the SMC. If so, it may be an H II region or a supernova remnant, but it is difficult to be more definitive without having high-resolution data at other frequencies. Nevertheless, the absence of X-ray emission argues against an SNR identification though SNR 0101–7226 in the SMC is an SNR with no X-ray emission (Ye et al. 1995). The compact source is possibly a background source unrelated to the extended partial ring, although it could also be located within the SMC. These sources are probably unrelated but without further data no definitive conclusion can be made.

0032–738 The MOST image of this region is shown in Figure 4.10. There is a relatively strong source to the north-west of the image and a weaker, possibly unrelated source to the south-east.

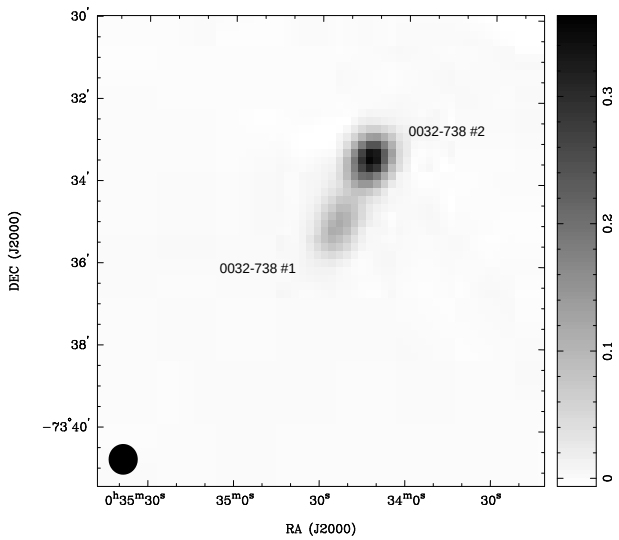

Figure 4.10: The MOST 843 MHz total intensity image of the field 0032–738 in the Small Magellanic Cloud. The intensity units are in Jy/beam.

Three sources were detected within the single ATCA field, and these are shown in separate subimages in Figure 4.11. The first of the three sources, ATCA 0032–738 #1, is elongated in the north-south direction. ATCA source 0032–738 #2 is unresolved. The final image of the group, ATCA 0032–738 #3, shows a relatively compact source to

the north-west with some suggestion of diffuse, extended emission towards the centre of the subimage, south-east of the compact source. The source parameters derived from the ATCA observations are given in Table 4.3.

The Parkes surveys detected a source B0032–7350 at all the observed frequencies and the results were consistent with the previous identification as a background source. All three ATCA sources are blended into the Parkes source and are further detailed in Table 4.3. No X-ray or infrared emission has been detected from these sources. Morphological considerations suggest that the first two ATCA images are probably background sources as these are compact at the resolution ATCA and do not appear to be associated with any other emission. ATCA source 0032–738 #3 is more interesting, particularly if the apparent faint, diffuse emission towards the centre of the subimage is real and associated with the slightly extended source to the north-west. More detailed observations will be required to determine if this source and/or the diffuse emission is in the SMC. It could be a background source with resolved radio lobes.

0036–746 A single compact source was detected in both the MOST and the ATCA images of this field, shown in Figure 4.12. The source position and flux densities are given in Table 4.3. There is excellent positional agreement at both observed radio frequencies and the source fitting procedure gives deconvolved source dimensions at both frequencies that are very close to those of a point source.

The Parkes survey source B0036–7438 has very good positional agreement with the ATCA determined position and is almost certainly the same source. Comparing the results in Tables 4.3 and 4.4 also reveals that the Parkes flux densities at 4.75 GHz and 4.85 GHz are similar to that determined from the ATCA 4790 MHz data. The Parkes values are slightly higher than the ATCA, consistent with the significantly larger beamwidth at Parkes. Again, no X-ray or infrared emission has been detected from this position. Based on these considerations, this is likely to be a compact background source.

0037–719 and 0038–720 A single MOST image centered on 0035–711 shows three compact sources with no apparent extended emission. This combined field is shown in Figure 4.13. Two of these sources were observed in a single ATCA field 0037–719, and the third in ATCA field 0038–720.

The two sources detected in the ATCA field are shown in Figure 4.14. The first image, source ATCA 0037–719 #1, shows a compact source with the suggestion of a narrow, linear region of slightly enhanced emission to the north-west of the subimage. The image of ATCA source 0037–719 #2, shows a compact source which is slightly elongated in the north-south direction but has no other significant features. The ATCA determined positions of the compact components are given in Table 4.3.

As noted from the fitted source positions, there is a separation in declination of around 4 arcmin thus allowing for the possible identification of two distinct sources from the Parkes surveys. Parkes source B0037–7152 is located just over 1 arcmin from the ATCA position and was previously identified as a background source. There is no X-

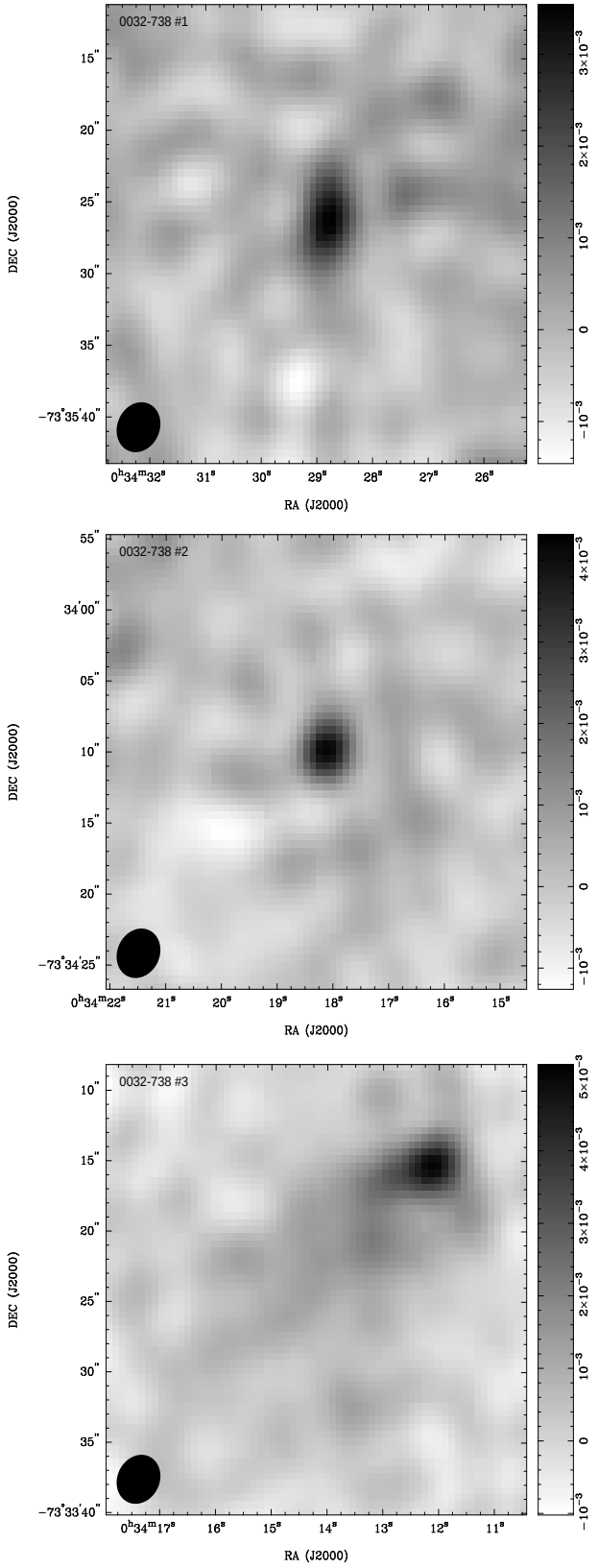

Figure 4.11: The ATCA 4790 MHz total intensity images of 0032-738 in the Small Magellanic Cloud. The intensity units are in Jy/beam.

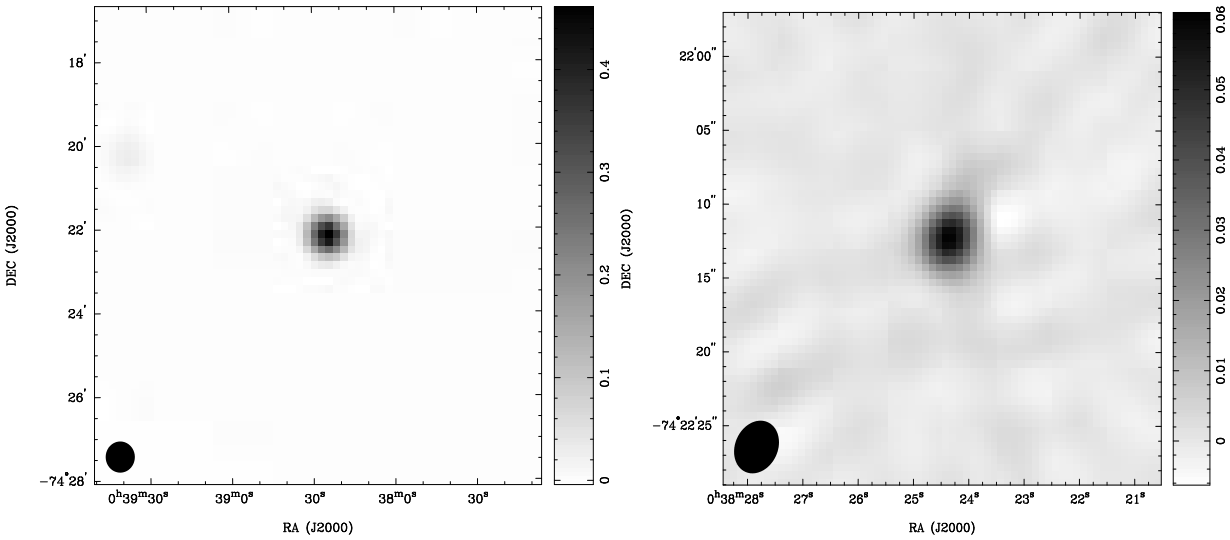

Figure 4.12: The MOST 843 MHz (left) and ATCA 4790 MHz (right) total intensity images of 0036–746 in the Small Magellanic Cloud. The intensity units are in Jy/beam.

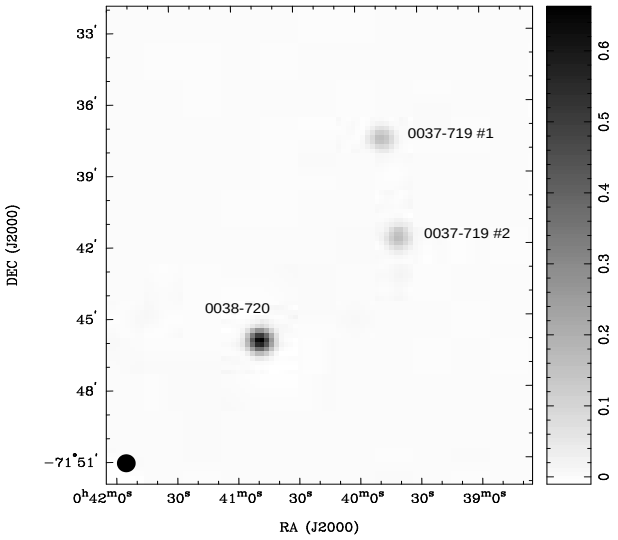

Figure 4.13: The MOST 843 MHz total intensity image of the ATCA fields 0037–719 and 0038–720 in the Small Magellanic Cloud. The strongest source in this image is the source in the field 0038–720. The two fainter sources are those mentioned in the discussion of the 0037–719 field. The intensity units are in Jy/beam.

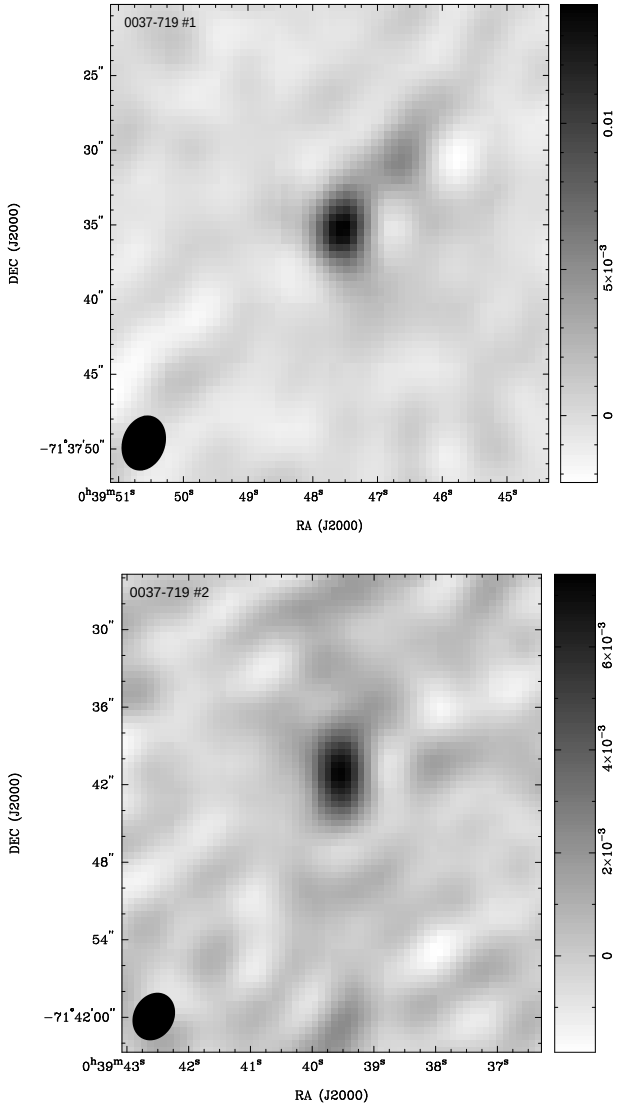

Figure 4.14: The ATCA 4790 MHz total intensity images of the field 0037–719 in the Small Magellanic Cloud. The intensity units are in Jy/beam.

ray or infrared emission from this region. It is most likely a background source although the diffuse emission observed with the ATCA, if real, could be located within the SMC. The Parkes Survey source B0037–7158 lies within 30 arcsec of the ATCA determined position and was previously catalogued as a background source. The nearest X-ray position, as determined by Kahabka et al. (1999), is just over 11 arcmin from the ATCA position so it is unlikely that this X-ray emission is from the same object observed in the radio. No coincident infrared emission is detected. These observations appear to support the accepted view that this object is a background source.

Figure 4.15 shows the only ATCA source in this field; it is a compact source with little or no extension. Nevertheless, the source fitting procedure successfully deconvolved this source into a gaussian with major and minor axes of 1.4×6.3 arcsec. The source position and flux density is given in Table 4.3. This source is the strongest feature in the MOST image shown in Figure 4.13 and has a flux density of almost 700 mJy at 843 MHz.

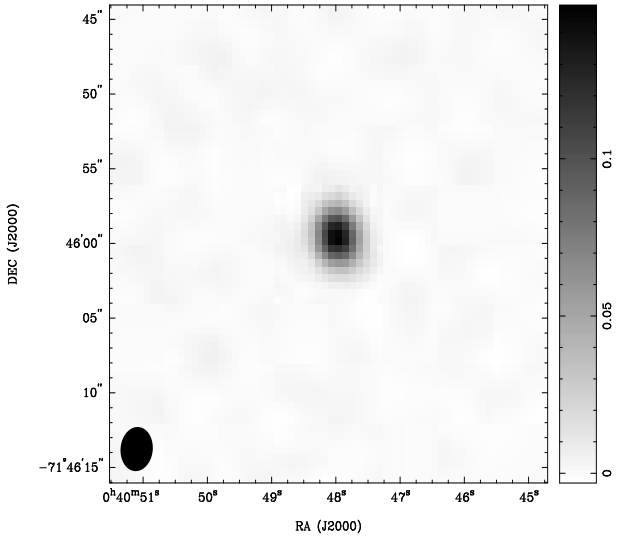

Figure 4.15: The ATCA 4790 MHz total intensity image of 0038-720 in the Small Magellanic Cloud. The intensity units are in Jy/beam.

Not surprisingly for a source with a flux density of 182 mJy at 5 GHz, a coincident radio source was detected at all observed centimetre wavelengths in the Parkes surveys. The positional agreement between the ATCA source at 4790 MHz and Parkes source B0037–7202 at 4.85 GHz is excellent, with the discrepancy less than 10 arcsec. In addition, the flux density at 4.85 GHz is 170 mJy which compares well with the integrated flux density obtained from the ATCA data. There is no detection at X-ray or infrared frequencies. These results support the previous identification by Ye (1988) that this source is a background source.

0041–709 The MOST and ATCA images of this field are shown in Figure 4.16. The morphology of the ATCA source strongly suggest that it is a radio galaxy and

extragalactic to the SMC. The MOST source also shows a slight extension along the SE-NW axis, which agrees with the morphology of the ATCA source. Clearly the standard gaussian source-fitting procedure used for compact sources is not appropriate for this object. The ATCA source positions determined from the peak pixel values are given in Table 4.3. A comparison of these positions with the multi-frequency Parkes survey data (Filipovic et al. 1997), suggest that the ATCA source and the Parkes source B0041–7057 may be the same object. This is consistent with the fact that B0041–7057 is classified as a background source by Filipovic et al. (1998b), although previous surveys had not classified it as a background source. A simple determination of the peak pixel value of each "lobe" of the source gives flux densities of approximately 25 mJy (NW) and 30 mJy (SW).

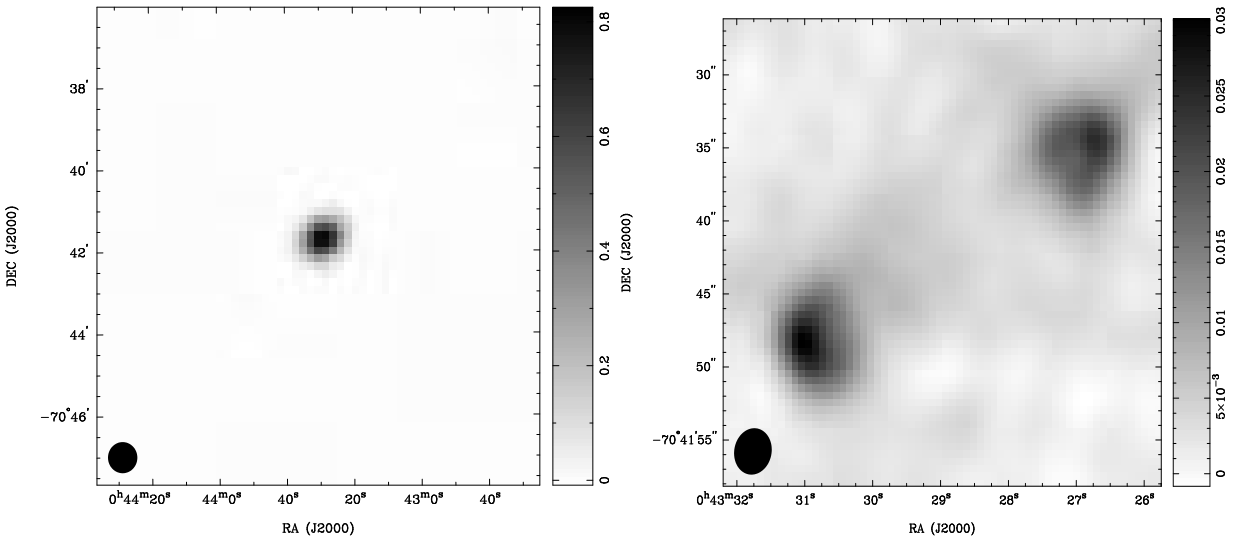

Figure 4.16: The MOST 843 MHz (left) and ATCA 4790 MHz (right) total intensity images of 0041–709 in the Small Magellanic Cloud. The intensity units are in Jy/beam.

A more accurate value of integrated flux density (and other image statistics) can be obtained by interactively selecting the region over which the flux density should be determined. The *MIRIAD* task `cgcurs` allows an arbitrary polygon to be defined and image statistics such as integrated flux density and flux weighted source position to be calculated. The values for the ATCA source given in Table 4.3 have been calculated in this fashion. The flux densities from the Parkes surveys (at 4.75 and 4.85 GHz) are around 200 mJy which is around the flux density of 264 mJy obtained from the ATCA observations at 4790 MHz. No X-ray or infrared emission associated with this source has been detected. It is highly probable that this is a radio galaxy behind the SMC.

0050–727 This source is located in the upper-right quadrant of the MOST image shown in Figure 4.1.

The ATCA image of the region near 0050–727 is shown in Figure 4.17. It reveals

two relatively compact sources that appear almost adjacent to each other. It is likely that this is just coincidence with each source being at a different distance.

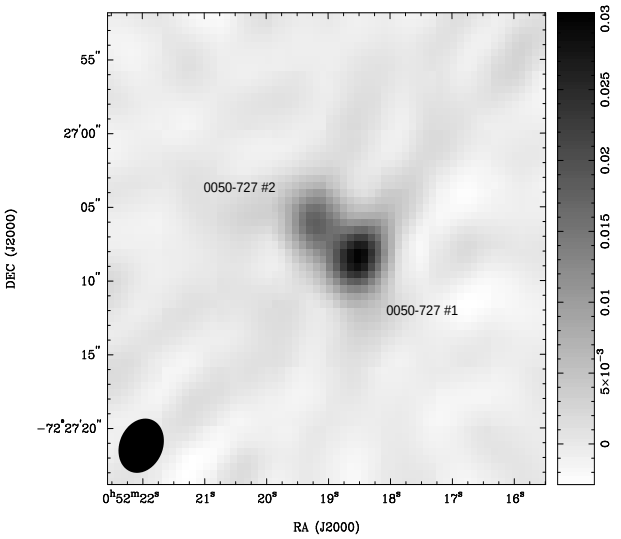

Figure 4.17: The ATCA 4790 MHz total intensity image of 0050–727 in the Small Magellanic Cloud. The intensity units are in Jy/beam.

The standard source-fitting procedure does not give meaningful results; in this case because these sources are so close to each other it effectively tries to fit a single gaussian to what would be better modelled by two gaussians. A similar procedure to that used for 0041–709 was therefore adopted in this case and the results presented in Table 4.3. The peak flux densities obtained from the maximum pixel value for each source are 30.4 mJy/beam and 18.5 mJy/beam. The integrated flux densities are obtained by interactively defining the region of interest, treating the sources individually, are given in Table 4.4. The nearest source in the Parkes survey is B0050–7301 which is over 15 arcmin away from the ATCA sources and therefore is most likely a different object. The ATCA sources can therefore be considered as new detections, and are most likely distinct background sources behind the SMC.

0054–713 Figure 4.18 shows the MOST 843 MHz and ATCA 4790 MHz images of this field. Both images are dominated by a single relatively strong, compact source. There is a faint but complete ring of emission around the source on the MOST image (more clearly seen on a display device), which is likely to be the first sidelobe that hasn't been fully removed during deconvolution. The MOST source has a deconvolved size which is only a few arcseconds larger than the synthesized beam. Applying the standard fitting procedure to the ATCA data flags this as a point source (i.e. the major and minor axes have similar extent to the synthesized beam). The source parameters are given in Table 4.3.

It is not surprising that for a source of this intensity, 214 mJy at 4790 MHz, there is an apparently coincident Parkes source, B0054–7123, detected at a range of frequencies

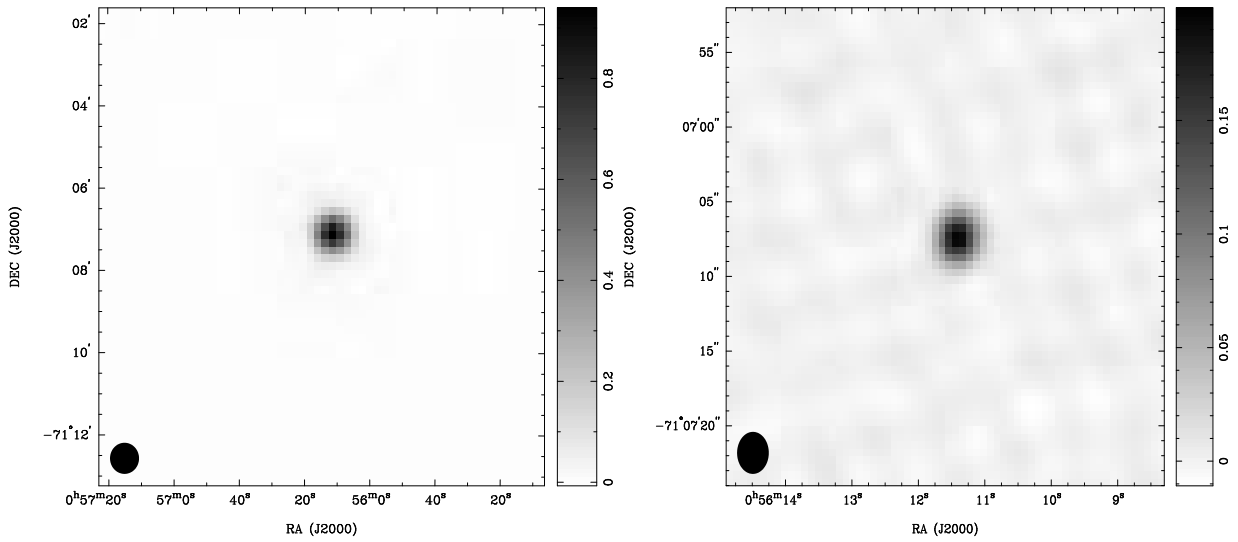

Figure 4.18: The MOST 843 MHz (left) and ATCA 4790 MHz (right) total intensity images of 0054–713 in the Small Magellanic Cloud. The intensity units are in Jy/beam.

as shown in Table 4.3. It has been classified by Filipovic et al. (1998b) as being a previously identified background source. The integrated ATCA flux density of 214 mJy compares favourably with the two Parkes values of 267 mJy and 224 mJy at similar observing frequencies, particularly given the difference in beamwidth. There is no X-ray or infrared emission detected from this region. These observations confirm the previous identification of this object as a background source.

0055–744 As for the previous field, the MOST and ATCA images of 0055–744 shown in Figure 4.19 show a single, relatively strong compact source only slightly larger than the synthesized beams. The source parameters are given in Table 4.3.

As this source is relatively strong the coincidence with the Parkes multi-frequency surveys is good; the ATCA and MOST positions are coincident with the Parkes source B0055–7429 (within the uncertainty of the Parkes beamwidth). B0055–7429 is classified as a background source. No X-ray or infrared emission has been detected from this region. A comparison of the flux density supports the fact that these sources are the same object. The ATCA 4790 MHz integrated flux density of 86 mJy and the two Parkes values of 92 mJy and 93 mJy at 4.75 GHz and 4.85 GHz respectively are in good agreement. Thus it is most likely that this is a background source.

0058–719 The MOST image of this field in Figure 4.20 shows a point-like source with an integrated flux density of approximately 200 mJy. There is some diffuse extended emission near the north edge of the image. The ATCA image suggests the presence of a slightly extended source at 4790 MHz.

The nearest source in the Parkes surveys is B0058–7154 which was only detected at 8.55 GHz with a flux density of 75 mJy. B0058–7154 was classified from previous

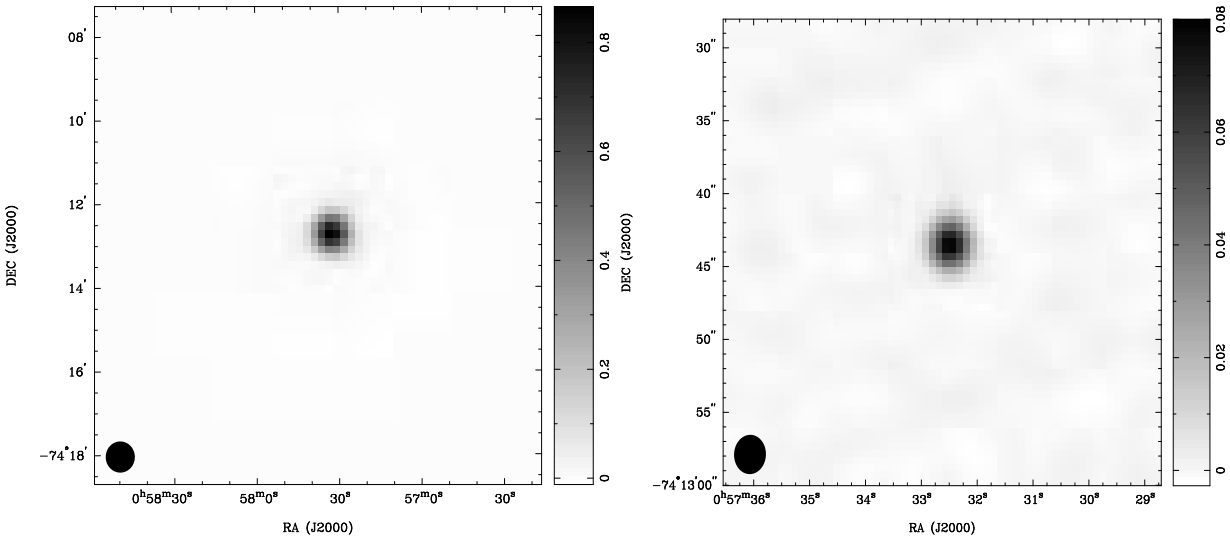

Figure 4.19: The MOST 843 MHz (left) and ATCA 4790 MHz (right) total intensity images of 0055–744 in the Small Magellanic Cloud. The intensity units are in Jy/beam.

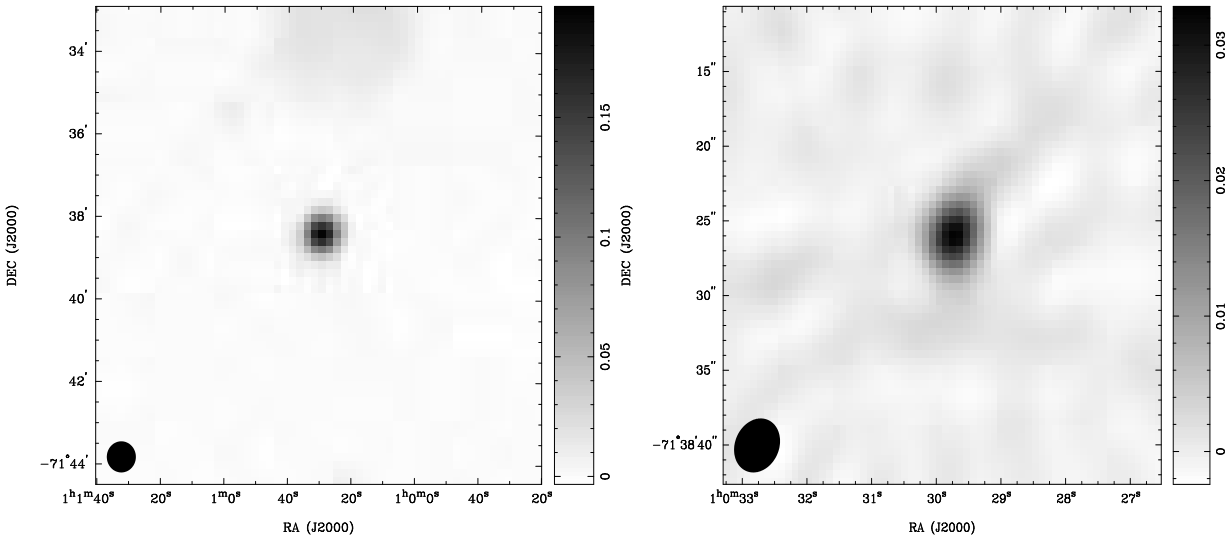

Figure 4.20: The MOST 843 MHz (left) and ATCA 4790 MHz (right) total intensity images of 0058–719 in the Small Magellanic Cloud. The intensity units are in Jy/beam.

surveys as a background source and has no associated infrared emission. The nearest X-ray source detected in the survey of Kahabka et al. (1999) is some 11 arcmin away in declination although there is good agreement in right ascension. It is highly unlikely that this X-ray source is related to the radio sources. This is consistent with the conclusion that this object is also a background source.

0107–718 The MOST image in Figure 4.21 shows a fairly compact source (with some slight extension to the south-west) with a few other weaker sources in this field. On the other hand the ATCA image shows two compact sources. Although nearby, they are likely to be unrelated. The parameters of both sources determined from the fitting procedure are given in Table 4.3.

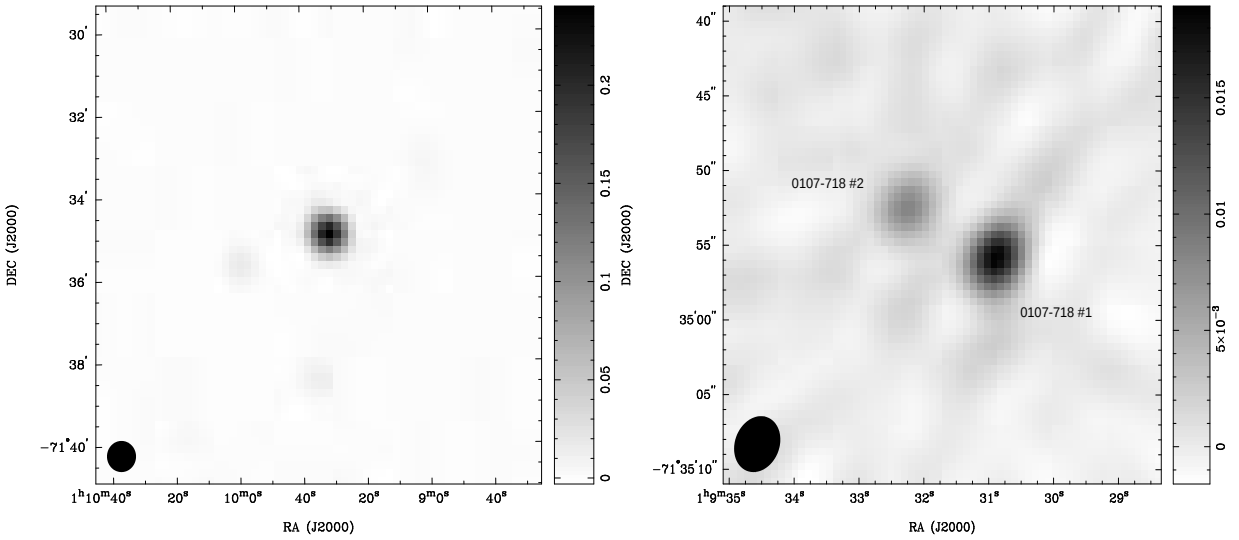

Figure 4.21: The MOST 843 MHz (left) and ATCA 4790 MHz (right) total intensity images of 0107–718 in the Small Magellanic Cloud. The intensity units are in Jy/beam.

The Parkes source B0108–7151, which is classified as extended at 2.45 GHz and 8.55 GHz, may be coincident with these sources. As can be seen from the source positions presented in Table 4.3, there are significant differences in the source positions at the various frequencies. Certainly source extension makes determination of an accurate position difficult but it is somewhat surprising that there is over 1 arcmin difference between the Parkes position at 1.42 GHz (where the source is *not* marked as being extended) and that at 8.55 GHz (where the source is marked as being extended). As the observing frequency increases, the beam size decreases so it could reasonably be expected that the more accurate position would be that obtained at the higher frequency.

Furthermore, the flux densities at the three lower frequencies decrease as the frequency increases, whereas the 8.55 GHz flux density is roughly twice that at 4.85 GHz. This may be due to intrinsic variability. However, the position differences and the

unusual spectrum raise doubts as to whether the Parkes survey results are actually for the same object and certainly no strong claim can be made that there is a definite association between the ATCA sources and B0108–7151. No X-ray or infrared emission has been detected from this region. It is probable that the two sources in the ATCA image are unrelated background sources.

0109–727 The MOST image shown in Figure 4.22 shows two sources that could be either a single source with an interesting morphology, or two distinct sources. The corresponding ATCA image in Figure 4.22 shows a single, strong compact source within the field which corresponds to the compact source in the centre of the MOST image. The elongated source seen on the MOST image is only marginally detected with the ATCA. It is almost resolved out at the angular resolution of the ATCA and is not shown here. The source-fitting deconvolution of the ATCA data indicates that this feature has similar dimensions to a point-source. The source parameters are given in Table 4.3. For the MOST data the integrated flux density was determined by interactively selecting a polygonal region which encompassed both sources using the *MIRIAD* task `cgcurs`.

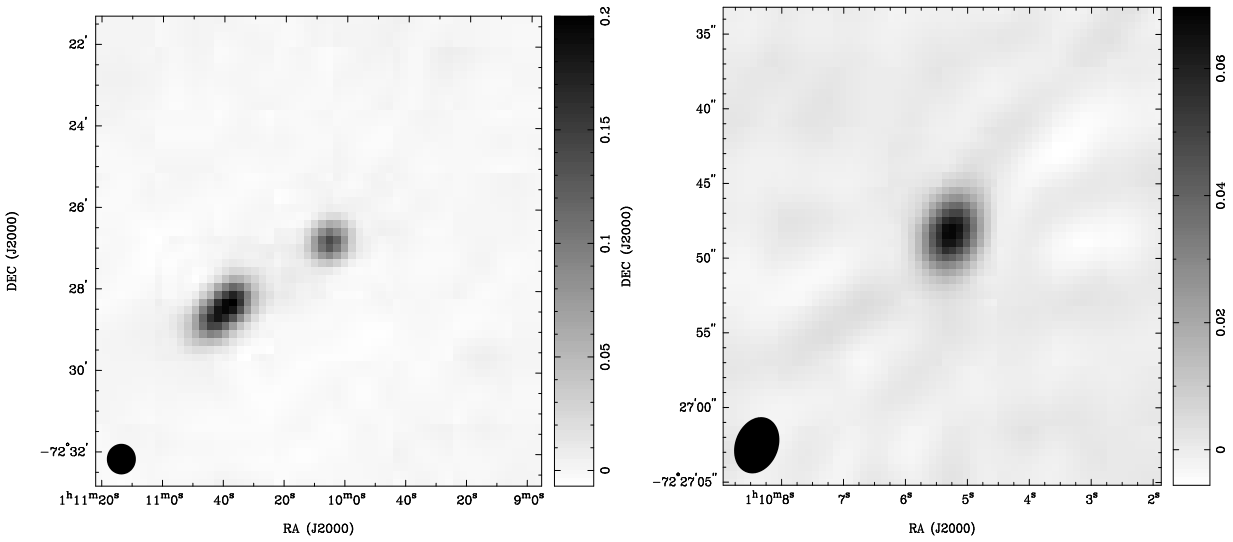

Figure 4.22: The MOST 843 MHz (left) and ATCA 4790 MHz (right) total intensity images of 0109–727 in the Small Magellanic Cloud. The intensity units are in Jy/beam.

The closest source from the Parkes survey is B0108–7243 whose position is given in Table 4.3. There is reasonable agreement between the ATCA and Parkes source positions. Filipovic et al. (1998b) identifies the Parkes source as being the known H II region, DEM S136. The flux density observed with the ATCA is significantly lower than the Parkes values at 4.75 GHz and 4.85 GHz but this can probably be explained by the fact that the ATCA was not sensitive to the larger-scale extended thermal emission. Furthermore, the MOST image doesn't indicate any significant diffuse and/or extended emission. No X-ray or infrared emission was detected from this area. It is probable

that the source observed with the ATCA (and the MOST) is a compact background source coincident with the H II region.

0109–735 Both the MOST and ATCA images of this field shown in Figure 4.23 indicate a relatively compact source. The MOST image clearly shows an elongated extension to the north-east, consistent with the suggestion of a faint, extended region to the east and north of the compact source visible in the ATCA image. Although only marginally visible in this version of the ATCA figure, viewing the same image on a display and interactively adjusting the lookup table indicates that the stronger the two "extensions" is to the east with a weaker area of emission to the north-east of the central component. Source position and flux density are given in Table 4.3.

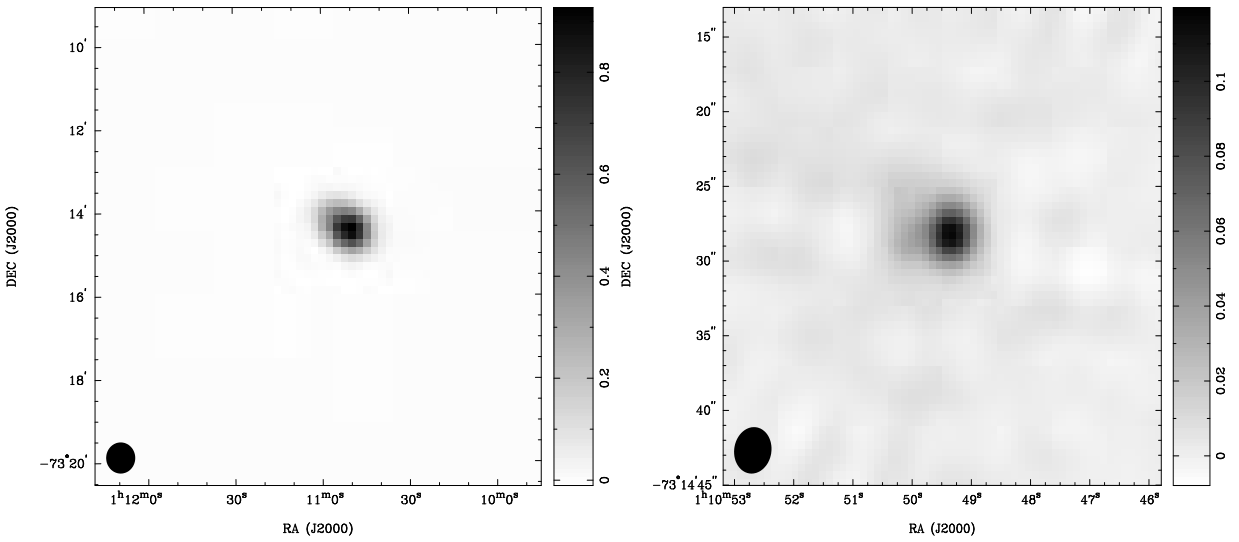

Figure 4.23: The MOST 843 MHz (left) and ATCA 4790 MHz (right) total intensity images of 0109–735 in the Small Magellanic Cloud. The intensity units are in Jy/beam.

Filipovic et al. (1998b) identifies the Parkes survey source B0109–7330 as being a previously identified background source. The positional agreement between the ATCA source and B0109–7330, particularly at the higher Parkes frequencies, is very good. The difference is less that 10 arcsec for the most accurate 6 and 3 cm Parkes positions. An integrated flux density of around 200 mJy was determined from the source-fit to the ATCA data. This compares relatively well with a flux density of 237 mJy obtained from the 4.75 GHz Parkes observations. Neither of these values are similar to the 4.85 GHz value of 319 mJy obtained in PMN survey (Wright et al. 1994). As for many of the other sources observed in this programme, no X-ray or infrared emission has been detected. The faint, extended emission observed with the MOST and ATCA may be located within the SMC itself, although it could be associated with the compact background source.

0131–729 The MOST image in Figure 4.24 shows a compact source with dimensions comparable to that of the synthesized beam. As for the ATCA data shown in the same figure, a single, slightly extended but relatively compact source is observed. Source position, peak and integrated flux density are given in Table 4.3.

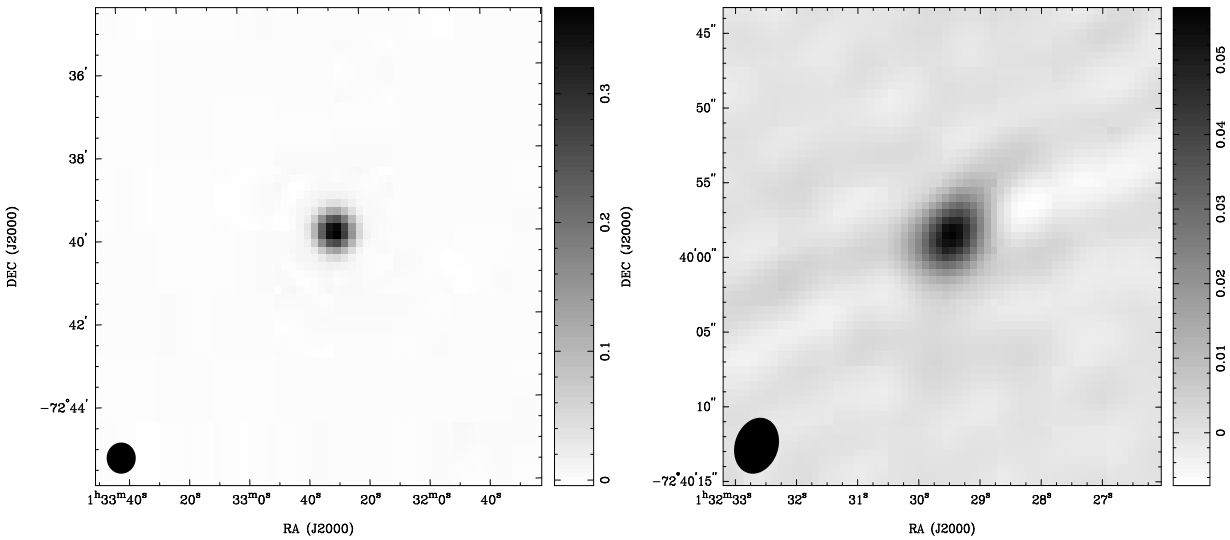

Figure 4.24: The MOST 843 MHz (left) and ATCA 4790 MHz (right) total intensity images of 0131–729 in the Small Magellanic Cloud. The intensity units are in Jy/beam.

The Parkes survey source B0131–7255 is a strong candidate for identification with this ATCA source. Positional agreement is good with a difference of less than 20 arcsec at 6 cm. The integrated flux density of the ATCA source is around 80 mJy. This is quite different to the Parkes 4.75 GHz value of 113 mJy but agrees well with the PMN survey value of around 74 mJy. This relationship is opposite to that found for the source 0109–735 which may indicate some intrinsic variability or uncertainty in measurement. No X-ray or infrared emission was detected from this region. The source was identified previously as a background source, and these observations support that identification.

Table 4.3: Comparison of the MOST 843 MHz, ATCA 4790 MHz and X-ray observations of compact sources in the Small Magellanic Cloud with published Parkes Survey Data. The reference column indicates if the tabulated data was taken from a published survey.

Source	Frequency (GHz)	Source Position (B1950.0)	Source Position (J2000.0)	Integrated Flux Density (mJy)	Reference/ Notes
0021–742					
MOST #1	0.843		00 24 10.65 –73 57 15.1	318	
MOST #2	0.843		00 23 36.17 –73 55 29.1	440	
ATCA #1	4.79		00 24 11.78 –73 57 18.0	53	
ATCA #2	4.79		00 23 35.74 –73 55 28.6	171	
B0022–7403	4.85	00 22 28.2 –74 03 11	00 24 38.2 –73 46 34	44	Filipovic
B0021–7412	1.42	00 21 48.7 –74 13 09	00 23 59.1 –73 55 31	554	Filipovic
B0021–7412	2.45	00 21 38.5 –74 12 19	00 23 49.1 –73 55 42	262	Filipovic
B0021–7412	4.75	00 21 43.7 –74 12 11	00 23 54.2 –73 55 34	102	Filipovic
B0021–7412	4.85	00 21 37.9 –74 12 12	00 23 48.5 –73 55 35	156	Filipovic
0032–738					
MOST #1	0.843		00 34 23.77 –73 34 59.8	246	Weaker src
MOST #2	0.843		00 34 13.64 –73 33 27.6	560	Stronger src
MOST #3	0.843		00 34 13.64 –73 33 27.6	784	Entire region
ATCA #1	4.79		00 34 28.80 –73 35 26.2	6	
ATCA #2	4.79		00 34 18.10 –73 34 09.8	5	
ATCA #3	4.79		00 34 12.45 –73 33 16.4	28	
B0032–7350	1.42	00 32 17.1 –73 50 26	00 34 17.8 –73 33 54	411	Filipovic
B0032–7350	2.45	00 32 12.2 –73 50 01	00 34 13.0 –73 33 29	322	Filipovic
B0032–7350	4.75	00 32 14.8 –73 50 09	00 34 15.5 –73 33 37	140	Filipovic
B0032–7350	4.85	00 32 13.7 –73 50 38	00 34 14.4 –73 34 06	166	Filipovic
B0032–7350	8.55	00 32 13.2 –73 50 09	00 34 14.0 –73 33 37	111	Filipovic
0036–746					
MOST #1	0.843		00 38 24.59 –74 22 10.4	481	
ATCA #1	4.79		00 38 24.35 –74 22 12.2	69	
B0036–7438	1.42	00 36 29.0 –74 38 30	00 38 23.6 –74 22 01	384	Filipovic
B0036–7438	2.45	00 36 30.9 –74 38 30	00 38 25.4 –74 22 01	168	Filipovic
B0036–7438	4.75	00 36 36.4 –74 38 40	00 38 30.8 –74 22 11	74	Filipovic
B0036–7438	4.85	00 36 28.2 –74 38 40	00 38 22.8 –74 22 11	81	Filipovic
0037–719					
MOST #1	0.843		00 39 47.71 –71 37 34.4	171	
MOST #1	0.843		00 39 40.11 –71 41 43.3	193	
ATCA #1	4.79		00 39 47.52 –71 37 35.1	18	
ATCA #2	4.79		00 39 39.55 –71 41 40.9	13	
B0037–7152	4.75	00 37 04.0 –71 52 54	00 39 04.3 –71 36 25	58	Filipovic
B0037–7158	4.85	00 37 49.1 –71 58 38	00 38 30.8 –71 42 10	66	Filipovic
0039.5-7153	X-ray		00 39 35.5 –71 53 03	–	Kahabka
0038–720					
MOST #1	0.843		00 40 48.30 –71 45 59.2	687	
ATCA #1	4.79		00 40 47.97 –71 45 59.5	182	
B0038–7202	1.42	00 38 29.9 –72 01 45	00 40 28.6 –71 45 17	786	Filipovic
B0038–7202	2.45	00 38 37.9 –72 01 42	00 40 36.5 –71 45 14	394	Filipovic
B0038–7202	4.75	00 38 53.1 –72 02 07	00 40 51.5 –71 45 40	153	Filipovic
B0038–7202	4.85	00 38 50.3 –72 02 23	00 40 48.7 –71 45 56	170	Filipovic
B0038–7202	8.55	00 38 58.0 –72 02 04	00 40 56.3 –71 45 37	147	Filipovic

Table 4.3: (continued)

Source	Frequency (GHz)	Source Position (B1950.0)	Source Position (J2000.0)	Integrated Flux Density (mJy)	Reference/ Notes
0041–709					
MOST #1	0.843		00 43 28.97 –70 41 41.2	997	
ATCA #1	4.79		00 43 28.88 –70 41 41,4	264	
B0041–7057	1.42	00 41 36.1 –70 58 23	00 43 34.3 –70 41 58	669	Filipovic
B0041–7057	2.45	00 41 31.9 –70 57 56	00 43 30.2 –70 41 31	398	Filipovic
B0041–7057	4.75	00 41 25.8 –70 57 59	00 43 24.2 –70 41 34	218	Filipovic
B0041–7057	4.85	00 41 32.1 –70 57 55	00 43 30.4 –70 41 30	197	Filipovic
0050–727					
MOST #1	0.843		00 52 18.61 –72 27 06.0	334	
ATCA #1	4.79		00 52 18.53 –72 27 08.6	36	
ATCA #2	4.79		00 52 19.19 –72 27 06.1	21	
0054–713					
MOST #1	0.843		00 56 11.34 –71 07 06.8	996	
ATCA #1	4.79		00 56 11.41 –71 07 07.4	214	
B0054–7123	1.42	00 54 33.7 –71 23 27	00 56 20.3 –71 07 13	687	Filipovic
B0054–7123	2.45	00 54 20.8 –71 23 01	00 56 07.6 –71 06 47	410	Filipovic
B0054–7123	4.75	00 54 27.6 –71 22 58	00 56 14.3 –71 06 45	267	Filipovic
B0054–7123	4.85	00 54 23.7 –71 23 15	00 56 10.4 –71 07 01	224	Filipovic
0055–744					
MOST #1	0.843		00 57 32.49 –74 12 43.4	871	
ATCA #1	4.79		00 57 32.49 –74 12 43.4	86	
B0055–7429	1.42	00 56 02.4 –74 28 50	00 57 37.6 –74 12 38	500	Filipovic
B0055–7429	2.45	00 55 55.4 –74 29 34	00 57 30.7 –74 13 22	279	Filipovic
B0055–7429	4.75	00 56 08.6 –74 28 59	00 57 43.7 –74 12 47	92	Filipovic
B0055–7429	4.85	00 55 59.9 –74 29 05	00 57 35.2 –74 12 53	93	Filipovic
0058–719					
MOST #1	0.843		01 00 29.35 –71 38 24.3	196	
ATCA #1	4.79		01 00 29.72 –71 38 25.9	38	
B0058–7154	8.55	00 58 37.9 –71 54 27	01 00 19.5 –71 38 18	75	Filipovic
0100.4-7149	X-ray		01 00 26.6 –71 49 28	–	Kahabka
0107–718					
MOST #1	0.843		01 09 31.50 –71 34 53.0	258	
ATCA #1	4.79		01 09 30.89 –71 34 55.7	20	
ATCA #2	4.79		01 09 32.25 –71 34 52.4	9	
B0108–7151	1.42	01 07 41.3 –71 51 57	01 09 15.5 –71 35 59	466	Filipovic
B0108–7151	2.45	01 07 56.6 –71 51 45	01 09 30.6 –71 35 47	234	Filipovic
B0108–7151	4.85	01 08 02.8 –71 51 15	01 09 36.7 –71 35 17	106	Filipovic
B0108–7151	8.55	01 08 08.2 –71 50 55	01 09 42.1 –71 34 57	218	Filipovic
0109–727					
MOST #1	0.843		01 10 39.39 –72 28 30.6	578	
ATCA #1	4.79		01 10 05.27 –72 26 48.3	74	
B0108–7243	1.42	01 09 07.4 –72 43 54	01 10 37.2 –72 27 58	514	Filipovic
B0108–7243	2.45	01 08 49.3 –72 43 24	01 10 19.4 –72 27 27	350	Filipovic
B0108–7243	4.75	01 08 56.2 –72 43 40	01 10 26.1 –72 27 43	157	Filipovic
B0108–7243	4.85	01 08 49.2 –72 43 45	01 10 19.2 –72 27 48	123	Filipovic

Table 4.3: (continued)

Source	Frequency (GHz)	Source Position (B1950.0)	Source Position (J2000.0)	Integrated Flux Density (mJy)	Reference/ Notes
0109–735					
MOST #1	0.843		01 10 51.16 –73 14 23.4	945	
ATCA #1	4.79		01 10 49.42 –73 14 28.1	198	
B0109–7330	1.42	01 09 21.5 –73 30 08	01 10 47.9 –73 14 12	1418	Filipovic
B0109–7330	2.45	01 09 25.0 –73 30 01	01 10 51.4 –73 14 05	656	Filipovic
B0109–7330	4.75	01 09 27.5 –73 30 20	01 10 53.8 –73 14 24	237	Filipovic
B0109–7330	4.85	01 09 22.0 –73 30 18	01 10 48.4 –73 14 22	319	Filipovic
B0109–7330	8.55	01 09 23.2 –73 30 19	01 10 49.6 –73 14 23	210	Filipovic
0131–729					
MOST #1	0.843		01 32 29.60 –72 39 55.3	393	
ATCA #1	4.79		01 32 29.48 –72 39 58.5	79	
B0131–7255	1.42	01 31 22.2 –72 53 51	01 32 31.8 –72 38 28	386	Filipovic
B0131–7255	2.45	01 31 16.3 –72 55 19	01 32 25.9 –72 39 56	175	Filipovic
B0131–7255	4.75	01 31 16.9 –72 55 04	01 32 26.5 –72 39 41	113	Filipovic
B0131–7255	4.85	01 31 16.0 –72 55 14	01 32 25.6 –72 39 51	74	Filipovic

4.3 Source Categorization

The observational data presented, and the comparison with existing published catalogues, suggest that most of the observed sources are likely to be external to the SMC. Even the compact sources that appear to be coincident with, or embedded in, regions of extended emission are likely to be "background" objects that happen to be coincident with objects within the SMC. This result is not surprising given that the selected sources were compact or only slightly extended at 843 MHz. Nevertheless, many apparently single sources in the MOST images were resolved into multiple compact sources at the higher resolution of the ATCA.

4.3.1 Source Statistics

Some details on radio source counts applied to MOST data have been given in Chapter 3 in which the derivation of the $\log N/\log S$ curve is discussed.

The MOST survey of the Small Magellanic Cloud covers an area of approximately 20 square degrees. The source selection used a flux density limit of around 200 mJy at 843 MHz (although a number of sources have flux densities slightly lower than this). The expected background source count for this cutoff is 1.1 sources/sq. deg which suggests around 22 sources should be detected in the 20 square degrees covered in the SMC. This is the number of sources that could reasonably be detected (given the constraints of the model) with the MOST in the direction of the SMC if the SMC was not present. Thus it provides an indicative count of the number of expected "background" sources that could be detected.

The results presented in Table 4.4 suggest that there are 17 MOST sources that have integrated flux densities ≥ 200 mJy, and a further three sources with flux densities between 170 and 200 mJy. This compares well with the expected value, especially

considering that this sample was not expected to be complete, and given an estimated 10% uncertainty in the flux densities.

The Parkes-Tidbinbilla Interferometer Data

Observations with the Parkes-Tidbinbilla Interferometer can be used to classify more definitely a source as being background to the SMC or otherwise.

A total of 15 SMC sources were observed with the PTI at 2290 MHz, and the results are presented in Table 4.4. The observations have been classified by inspection of amplitude as a function of fringe frequency and to a lesser extent by inspection of phase as a function of fringe frequency. Those sources which were fully resolved at this resolution are denoted by "ND" (for no detection) and those for which there is a potential marginal detection are indicated by a question mark. Some sources have multiple, distinct components and in this case the pseudo flux density is given for each component. For two objects, complex structure is observed in the fringe amplitude. The data have only been approximately amplitude calibrated, and the flux density is accurate to within 10-20% of the true value.

A PTI detection requires that a source has a high apparent brightness and very small angular extent. Those sources detected with the PTI in this study are likely to be located behind the SMC. However, the possibility remains that such an object could be located in the SMC, and if this was the case it would be an extremely interesting source for further study. Although the known H II regions N83/N84 and N90 have associated PTI detections it would seem likely that there are also background sources that are coincident with these regions. The images from the MOST, particularly of N83/N84, show clearly a number of relatively strong compact sources at the position of the H II region. The other seven sources which were detected with the PTI were classified as background sources based on the MOST and ATCA data presented here and from previously published Parkes single-dish multi-frequency data.

Although most of these SMC sources are "behind" the SMC and may be the central cores of distant radio galaxies, quasars or other distant extragalactic objects, at least a few of these "background" sources may be located in the SMC itself. Further data and a deeper understanding are required to distinguish these two classes with certainty.

4.3.2 Radio Spectral Index

A common method of classifying and categorizing sources is based on their spectrum. Many radio sources have a spectrum which is well fitted by a power law of the form $S \propto \nu^{+\alpha}$, where α is the spectral index.

Using data from observations in the direction of the LMC, McGee & Newton (1972), classified sources into three groups based in their spectral index as follows:

- $-1.8 < \alpha < -0.6$; background sources,
- $-0.8 < \alpha < -0.2$; supernova remnants with a steep spectrum, and

Table 4.4: A comparison of integrated flux densities across a range of frequencies for the sources observed in the Small Magellanic Cloud. The 408 MHz data are taken from the Molonglo Reference Catalogue (i.e. data from the Mills Cross), the MOST 843 MHz values are from the data presented in this chapter as are ATCA 4790 MHz values (repeated from Tables 4.1, 4.2 and 4.3). The 2290 MHz values are from Parkes-Tidbinbilla Interferometer observations. Sources which are extended are indicated with (ext) and those which show extended and diffuse emission are marked with (ext/dif). ND indicates that the source was observed but not detected. Some PTI detections showed complex structure and this is indicated with (structure); a "?" indicates a marginal detection for which a fringe amplitude could not be easily determined.

Source	S_{408} (mJy)	S_{843} (mJy)	S_{4790} (mJy)	α	S_{2290} (pseudo mJy)
BKGS 7		53	ND		
BKGS 24		143	10	−1.5	
BKGS 32		66 (ext)	16	−0.8	
BKGS 33		62	12	−1.0	
N83/N84 #1		134	16, 18 & 8		30 & 25
N83/N84 #2		177	40		290
N90		214	73	−0.6	23 & 27
0021–742 #1	1160	414	53		?
0021–742 #2		529	17		?
0032–738 #1		246 (ext)	6		
0032–738 #2	1440	785 (ext)	5		
0032–738 #3		560 (ext)	28		
0036–746	830	481	69	−1.0	400
0037–719 #1		170	18		ND
0037–719 #2		193	13		ND
0038–720	930	687	182	−0.7	80
0041–709	1670	997 (ext)	264 (for region)		ND
0050–727		334	36 & 21		ND
0054–713	1440	996	214	−0.8	560 (structure)
0055–744	1800	925	86	−1.3	280
0058–719		204	38	−1.0	210 (structure)
0107–718		258 (ext/dif)	20 & 10		ND
0109–727		578 (ext)	74		340 & 90
0109–735	2270	1340 (ext)	198		15
0131–729		393 ???	79	−0.9	ND

- $\alpha > -0.2$; H II regions with a flat spectrum, or filled-centre SNRs.

Although derived from Large Cloud observations it is reasonable to expect that the statistical results would be similar for observations of the SMC (although a smaller total source count would lead to greater statistical uncertainty).

Filipovic et al. (1998b) used McGee and Newton's criteria as the basis for defining a more precise categorization. A histogram of spectral index versus number of sources was plotted for each source category (e.g. known H II regions), and from these a mean spectral index was determined for each category.

Filipovic found that the H II regions have essentially a flat spectrum, the known SNRs have a spectral index of $\alpha = -(0.22 \pm 0.07)$ and the background sources have a mean spectral index of $\alpha = -(0.45 \pm 0.06)$. The largest uncertainly is with the determination of the spectral index of the background sources. The authors attribute this to either the "background" source group being sub-divided into two distinct classes of flat and steep spectrum sources or due to intrinsic source variability particularly as the observations were undertaken over a number of years.

The small number of SMC source observations reported here, and the even smaller subset for which reliable spectral indices could be calculated, precludes a statistical study. Nevertheless, a number of conclusions can be drawn.

Caution must be exercised in the determination of the flux density used to calculate the spectral index. A deep understanding of the observing procedure and the sampling of spatial frequencies is necessary in order to determine whether the calculated spectral index is astrophysically significant. For example, a source which is compact at the resolution of the MOST may be resolved into subcomponents (because of the lack of sensitivity to larger-scale structure) when observed with higher angular resolution with the ATCA. The ATCA, in common with other interferometers, may not accurately image extended structure which corresponds to an angular extent equal to or larger than the shortest baseline.

The spectral index for ten sources observed in this programme have been calculated and included in Table 4.4. These sources were selected on the basis of their simple morphology and the dimensions determined from the source fitting procedure. The criterion used was to select only those sources which appeared to be of similar dimensions to the synthesized beam, were not located within areas where a number of sources had been detected and did not appear to be embedded in diffuse extended emission. Where 408 MHz data was available this was included in the calculation. In these cases the fit to the three data points was relatively good with the maximum uncertainly from the least squares fit being of the order of 0.1.

The flattest spectrum measured in the selected sample of MOST and ATCA SMC sources was $\alpha = -0.62$ with most in the range of -0.8 to -1.0. This is significantly different to the mean values determined in the work of Filipovic et al. (1998b). A possible reason for this is that a significant amount of thermal emission (from the Clouds themselves) may have been included in the larger Parkes beam, increasing the apparent flux density and causing the spectrum determined from these data to be artificially flattened. Similarly, the flux densities determined from the ATCA may not

represent the true flux density due to under-sampling, leading to a steeper apparent spectrum. The latter effect was minimized by choosing only those sources which had similar dimensions to that of the synthesized beam.

4.4 Summary

Throughout this chapter, images and corresponding analysis of a number of sources in the Small Magellanic Cloud have been presented. The number of sources observed in this programme compares well with the expected number of background sources in a complete sample.

It has been shown that even with multi-frequency and high angular resolution data, the classification and identification of sources is a complex process. One of the most commonly used classifications in radio astronomy is based on spectral index. Whilst this is certainly valid, particularly for some classes of objects, it should only be complemented by other methods for identifying sources and not relied on in isolation. The process is often complicated when trying to use flux densities determined from different instruments (which is often necessary in order to get a satisfactory frequency range). For the sources observed in this work, the spectral index has been used more as a further check of the earlier identification rather than as the absolute determination of source classification.

As expected, most of the sources reported on here are likely to be background objects located behind the SMC itself. These new data have served to either support previous identifications or make new ones. Reference to previously published optical, radio, X-ray and infrared catalogues has been used to aid in the source identification and classification where available. It would be extremely difficult (if not impossible) to obtain optical identifications of sources located behind the SMC.

A similar scenario is expected in the larger sample of sources observed in the direction of the Large Magellanic Cloud. These data are discussed in detail in the following Chapter.